

# On the precise measurement of the $X(3872)$ mass and its counting rate\*

Pablo G. Ortega<sup>1,†</sup> and Enrique Ruiz Arriola<sup>2,‡</sup>

<sup>1</sup>*Departamento de Física Fundamental and  
Instituto Universitario de Física Fundamental y Matemáticas (IUFFyM),  
Universidad de Salamanca, E-37008 Salamanca, Spain*

<sup>2</sup>*Departamento de Física Atómica, Molecular y Nuclear  
and Instituto Carlos I de Física Teórica y Computacional  
Universidad de Granada, E-18071 Granada, Spain.*

(Dated: December 7, 2020)

The lineshapes of specific production experiments of the exotic state such as  $X(3872)$  with  $J^{PC} = 1^{++}$  quantum numbers involving triangle singularities have been found to become highly sensitive to the binding energy of weakly bound states, thus offering in principle the opportunity of benchmark determinations. We critically analyze recent proposals to extract accurately and precisely the  $X(3872)$  mass, which overlook an important physical effect by regarding their corresponding production lineshapes as a sharp mass distribution and, thus, neglecting the influence of initial nearby continuum states in the  $1^{++}$  channel. The inclusion of these states implies an effective cancellation mechanism which operates at the current and finite experimental resolution of the detectors so that one cannot distinguish between the  $1^{++}$  bound-state and nearby  $\bar{D}D^*$  continuum states with the same quantum numbers. In particular, we show that the lineshape for resolutions above 1 MeV becomes rather insensitive to the binding energy unless high statistics is considered. The very existence of the observed bumps is a mere consequence of short distance correlated  $\bar{D}D^*$  pairs, bound or unbound. The cancellation also provides a natural explanation for a recent study reporting missing but unknown decay channels in an absolute branching ratio global analysis of the  $X(3872)$ .

PACS numbers: 12.39.Pn, 14.40.Lb, 14.40.Rt

Keywords: Triangle singularities, Charmed mesons, Exotic states

## I. INTRODUCTION

The quest for the hadronic spectrum has been a major goal in particle physics over the last 70 years, which has been marked by predicting and reporting the observed states and their properties in the PDG (see e.g. [1] for the latest edition upcoming). Before 2003, this task has mostly been phenomenologically supported by a non-relativistic quark model pattern and its given symmetry multiplets suggested by the underlying  $q\bar{q}$  and  $qqq$  composition for mesons and baryons, respectively. This non-rigorous but effective link has been a quite useful and extremely relevant guidance, particularly because, currently, it is theoretically unknown how many states should occur below a given maximal energy or if the full set of recorded states are incomplete or redundant [2]. In fact, as it is most often the case for hadronic resonances, we do not detect directly the reported particle through its track but only in terms of its decaying products so that the corresponding invariant mass distribution is observed instead and the relevant signal is singled out from the reaction background within a *given* energy resolution.

Since 2003, the situation has become more involved above charm production threshold after the discovery of the  $X(3872)$  [3–6] and the wealth of new  $X, Y, Z$  states whose properties suggest more complicated structures than those originally envisaged from the quark-model [7–9]. In this study, we analyze the renowned  $X(3872)$  state and the influence of the mass distribution in the  $1^{++}$  channel on the determination of its mass. The  $X(3872)$  is allegedly a  $\bar{D}D^*$  weakly bound state, whose binding energy has become smaller since its discovery. The most recent value for its binding energy, measured by LHCb, is 0.07(12) MeV [10] for a  $1\sigma$  confidence level. This actually corresponds to a 30% probability of *not* being a bound state. We illustrate the situation in Fig. 1 within a conventional Gaussian distribution profile interpretation. So, at present, it is unclear whether its mass is slightly above or below the  $\bar{D}D^*$  threshold. However, one might wonder what would happen if the  $X(3872)$  is not a bound state. Recently several proposals invoke the strong sensitivity of lineshapes for production processes involving triangle singularities to benchmark the mass determination [11, 12].

In this paper, we promote the idea that the precise value of the mass is actually not crucial, since the contribution of nearby states with the *same* quantum numbers is unavoidable with the current experimental energy resolution detecting its decaying products, and a cancellation mechanism put forward initially by Dashen and Kane [13] is at work in this particular case. We have found in previous works that this has implications to count  $X(3872)$  degrees of freedom at finite temperatures of relevance in relativistic heavy ions

\* This work is partly supported by the Spanish Ministerio de Economía y Competitividad and European ERDF funds (FPA2016-77177-C2-2-P, FIS2017-85053-C2-1-P), Junta de Andalucía (FQM-225) and by the EU STRONG-2020 project under the program H2020-INFRAIA-2018-1, grant agreement no.824093.

† pgortega@usal.es

‡ earriola@ugr.es

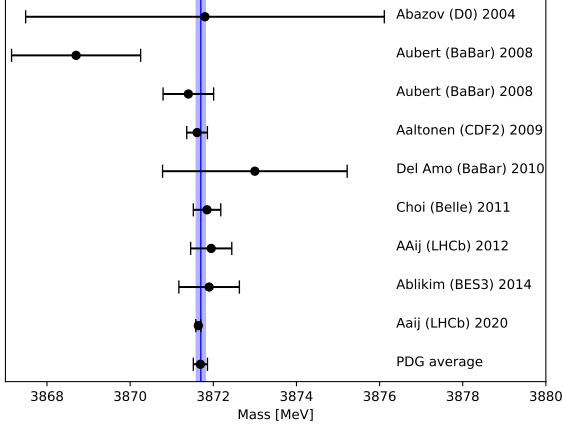


FIG. 1. Different  $X(3872)$  masses determinations [3–6] with standard 68% confidence limits. The band corresponds to the current  $\bar{D}D^*$  threshold value with uncertainties.

collisions [14, 15] and ultrahigh energies pp prompt  $X(3872)$  production at finite  $p_T$  and mid-rapidity [16]. We will also show how the number of reconstructed states representing the bound  $X(3872)$  is *smaller* than the truly produced ones due to a cancellation mechanism which will be explained below and which provides a natural understanding of the missing decay channels. A brief account and overview of the present study has already been advanced in conference proceedings [17].

The paper is organized as follows: In section II we review the hadronic density of states and its theoretical and experimental limitations as it will be a key element of our analysis. In section III we review the XYZ states to provide a broader perspective around the very special  $X(3872)$  exotic state. In section IV we approach the determination of the density of states in the  $1^{++}$  channel. Our main numerical results are discussed in section V. In section VI we ponder on the relevance of  $\bar{D}\bar{D}^*$  correlations, rather than binding, as the key behind the observed signals. Finally, our conclusions are presented in Section VII.

## II. HADRONIC DENSITY OF STATES

### A. General properties

For completeness, in this section we review some basic aspects of the hadronic density of states following some historical timeline, in a way that our points can be more easily presented and with the purpose of fixing the notation. The first quantum-mechanical attempt to determine the density of states within the quantum virial expansion was pioneered by Beth and Uhlenbeck in 1937, who computed the second virial coefficient as a function of temperature in terms of the two-body scattering phase shifts [18]. Only after 30 years, Dashen, Ma and Bernstein provided, in a seminal work, the link to the full S-matrix [19] which opened up the basis for the Hadron Resonance Gas (HRG) model for resonances [20], as well

as the notion of effective elementarity [21]. Based on these developments, Dashen and Kane promoted the natural idea of counting hadronic states at a typical hadronic scale. In terms of the corresponding density of states as a function of the invariant CM energy  $\sqrt{s}$  [13], we have

$$\rho(M) = \text{Tr} \delta(M - H_{\text{CM}}) = \sum_n \delta(M - M_n) \quad (1)$$

where  $H_{\text{CM}}$  is the intrinsic Hamiltonian and  $M_n$  the corresponding eigenvalues. We use here a bound state notation but, in practice, the continuum spectrum which will be of concern here implies a spectral integral which can be approximated by imposing a discretization approximation, such as placing the system on a sufficiently large box with finite volume. Unfortunately, while this is mathematically a well-defined quantity,  $\rho(M)$  cannot, in most cases, be computed or measured directly, but only through its coupling to external probes generating the production process. This effectively correspond to multiply by an observable  $\mathcal{O}(M)$  and superimpose the contributions in a given energy window. Another possibility is the coupling to a thermal heat bath where we take this observable to be a universal Boltzmann factor  $e^{-M/T}$ .

### B. The two-body case

The level density can be splitted into separate contributions according to the corresponding good quantum numbers. In the particular  $2 \rightarrow 2$  process (for a recent discussion of N-body and coupled channel aspects see e.g. Refs. [22, 23] and references therein) one has that the interacting cumulative number in a given channel in the continuum with threshold  $M_{\text{th}}$  is given as [24, 25] (for updated presentations see e.g. [26, 27])

$$\begin{aligned} \Delta N(M) &\equiv N(M) - N_0(M) \\ &= \sum_n \theta(M - M_n^B) + \frac{1}{\pi} \sum_{\alpha=1}^n [\delta_{\alpha}(M) - \delta_{\alpha}(M_{\text{th}})]. \end{aligned} \quad (2)$$

Here, we have separated bound states  $M_n^B$  explicitly from scattering states written in terms of the eigenvalues of the S-matrix, i.e.  $S = U \text{Diag}(\delta_1, \dots, \delta_n) U^\dagger$ , with  $U$  a unitary transformation for n-coupled channels. This definition fulfills  $N(0) = 0$ . In the single channel case, and in the limit of high masses  $M \rightarrow \infty$  one gets  $N(\infty) = n_B + \frac{1}{\pi} [\delta(\infty) - \delta(M_{\text{th}})] = 0$  due to Levinson's theorem. The opening of new channels and the impact of confining interactions was discussed in Ref. [28]. According to Dashen and Kane, some states may present a fluctuation at the hadronic scale so that their contribution cancels, so that the state *does not* count.

### C. Theoretical binning

From a purely theoretical side, a practical and numerical evaluation of the level density rests on the computation of the energy levels,  $M_n$ , as demanded by Eq. (1) which could, in principle, be evaluated with arbitrary precision. In practice,

this evaluation requires binning the spectrum with a given finite invariant mass resolution  $\Delta m$ , in which case only an averaged or coarse-grained value such as [13]

$$\bar{\rho}(M) = \frac{1}{\Delta m} \int_{M-\Delta m/2}^{M+\Delta m/2} \rho(m) dm \quad (3)$$

is obtained. On the theoretical side, a practical way of implementing this is by placing the system into a box of volume  $V$ , as it is the case in lattice QCD where one roughly has  $\Delta m \sim V^{-1/3}$ . This finite mass resolution effectively corresponds to a coarse graining in mass and should not have any sizable effect on the result, *unless* the true density of states presents large fluctuations on a smaller mass scale. With this viewpoint in mind, Dashen and Kane made the distinction between the original  $SU(3)$  multiplets and “accidental” states, i.e. those states which *do not* contribute when  $\Delta m$  is sufficiently large (presumably about the typical symmetry breaking multiplet splitting).

#### D. Experimental resolution

On the experimental side, the coarse-graining procedure corresponds to the finite energy resolution of the detectors, typically  $\sigma = 1 - 3 \text{ MeV}$  (see also the discussion below). The amount of inherent fluctuation is estimated by assuming that the formation of each charge carrier in the detector is a Poisson process. This average corresponds to use a Gaussian detector response function with  $\sigma$ -broadening,

$$R_\sigma(m, M) = \frac{1}{\sqrt{2\pi}\sigma} e^{-\frac{(m-M)^2}{2\sigma^2}} \quad (4)$$

so, we have [29]

$$\bar{\rho}_\sigma(M) = \int_{-\infty}^{\infty} R_\sigma(m, M) \rho(m) dm \quad (5)$$

The binning procedure implied by Eq. (3) may be added afterwards. Although it is innocuous for  $\Delta m \leq \sigma$ , it can have a sizable effect for  $\Delta m > \sigma$ .

#### E. The Dashen-Kane cancellation

The immediate consequence of the particular phase shift behavior follows from Eq. 2 at the density of states level, defined as

$$\rho(M) = \frac{d\Delta N(M)}{dM} = \sum_n \delta(M - M_n^B) + \frac{1}{\pi} \sum_{\alpha=1}^n \delta'_\alpha(M). \quad (6)$$

Assuming an experimental resolution  $R_\sigma(m, M)$ , the corresponding measured quantity for an observable depending on the invariant mass function  $O(M)$  is

$$O_{\text{meas}}(M) = \int_{-\infty}^{\infty} O(m) R_\sigma(m, M) \rho(m) dm. \quad (7)$$

Then, for a bin in the range  $(M - \Delta m/2, m + \Delta m/2)$ , it becomes

$$O_{\text{meas}} \equiv \frac{1}{\Delta m} \int_{M-\Delta m/2}^{M+\Delta m/2} O_{\text{meas}}(M') dM'. \quad (8)$$

In the single channel case, with phase shift  $\delta(M)$ , one has

$$O_{\text{meas}} = \mathcal{R}(M^B) O(M^B) + \frac{1}{\pi} \int_{-\infty}^{\infty} \mathcal{R}(m) O(m) \delta'(m) dm, \quad (9)$$

with  $\mathcal{R}(m) = \frac{1}{2\Delta m} \left[ \text{Erf} \left( \frac{m-M^B+\Delta m/2}{\sqrt{2}\sigma} \right) + \text{Erf} \left( \frac{M^B-m+\Delta m/2}{\sqrt{2}\sigma} \right) \right]$ . Which, for a decreasing phase-shift and for a smooth observable  $O(M)$ , points to a cancellation whose precise amount depends on the corresponding slope above threshold.

#### F. The deuteron state and the np continuum

The cancellation between the continuum and discrete parts of the spectrum was pointed out by Dashen and Kane long ago [13] (see also [30, 31] for an explicit picture and further discussion within the HRG model framework). A prominent example of such a cancellation discussed in these works corresponds to the deuteron, which is a neutron-proton  $1^{++}$  state weakly bound by  $B_d = 2.2 \text{ MeV} \ll m_p + m_n \sim 1980 \text{ MeV}$ . This effect can explicitly be observed in the np virial coefficient at rather low temperatures [32] (this work however fails to link the effect to the Dashen-Kane effect). While this cancellation is not exactly a theorem, it is an open possibility *a fortiori* whose verification depends on details of low energy scattering. We point out that the cancellation observed in the equation of state for nuclear matter at low temperatures where one has a superposition of states weighted by a Boltzmann factor [32] corresponds to a suppression of the occupation number in the  $1^{++}$  channel as compared to the deuteron case,  $N_{1^{++}} \leq N_d$ .

The case of the deuteron described above is particularly interesting for us here since it is extremely similar to the case of the  $X(3872)$ , with the important exception of the detection method of both states, as will be discussed below. In our previous work [14] we have shown how this cancellation can likewise be triggered at finite temperature  $T$  for the  $X(3872)$ , as it is the case in relativistic heavy ion collisions, since the partition function involves the folding of the Boltzmann factor,  $\sim e^{-\sqrt{p^2+m^2}/T}$  with the density of states, Eq. 6. Therefore, given these suggestive similarities, we have undertaken a comparative study of the deuteron *and*  $X(3872)$  production rates in pp scattering at ultra-high energies ( $\sim 7 \text{ TeV}$ ) in the observed  $p_T$  distributions in colliders, which provides a suitable calibration tool in order to see the effects of the cancellation due to the finite resolution  $\Delta m$  of the detectors signaling the  $X(3872)$  state and deciding on its bound state character [16].

### III. THE XYZ STATES

Nowadays, there is a strong theoretical and experimental evidence on the existence of loosely bound states near the charm threshold, originally predicted by Nussinov and Sidhu [33], as it seems to be confirmed now by the wealth of evidence on the existence of the  $X(3782)$ , re-named  $\chi_{c1}(3782)$ , state with binding energy  $B_X = 0.01(18)\text{MeV}$  [34], or  $0.07(12)\text{MeV}$  from recent LHCb measurements [10], and which has triggered a revolution by the proliferation of the so-called X,Y,Z states (for reviews see e.g. [8, 9, 35]). In the absence of electroweak interactions, this state has the smallest known hadronic binding energy and, for a loosely bound state, many properties are mainly determined by its binding energy [8] since most of the time the system is outside the range of the interaction.

In fact, the molecular interpretation has attracted considerable attention, but since this state is unstable against  $J/\psi\rho$  and  $J/\psi\omega$  decays, the detection of  $X(3782)$  relies on its decay channels spectra where the mass resolution never exceeds  $\Delta m \sim 1\text{--}2\text{MeV}$  [3–6] (see e.g. [36] for a graphical summary on the current spectral experimental resolutions). Therefore it is in principle unclear if one could determine the mass of the  $X(3782)$  or, equivalently, its binding energy  $\Delta B_X \ll \Delta m$  with such a precision, since we cannot distinguish sharply the initial state. While in most studies (see however [37]) the bound state nature is assumed rather than deduced, even if the  $X(3782)$  was slightly unbound the correlations would be indistinguishable in the short distance behavior of the  $D\bar{D}^{*0}$  wave function.

The discussion on  $X(3782)$  lineshapes started in Ref. [38] as a way to extract information on the binding. Triangle singularities are ubiquitous in weakly bound hadronic and nuclear systems [39] and arise when three particles in a Feynman diagram can simultaneously be on the mass shell. Their relevance in XYZ states has been pointed out [40] and their relation to unitarity has been emphasized [41, 42]. In fact, they have been put forward recently as a method to sensitively determine the X mass based on the theoretical line shape. The fall-off of the lineshape above the peak, rather than the actual position of the peak reflects rather well the binding energy [11, 12, 43].

F.-K. Guo has considered the effect of a short distance source (the specific process has not been specified) which generates a  $D^{*0}\bar{D}^{*0}$  pair in a relative S-wave and which eventually evolves into a  $X(3782) + \gamma$  final state [11]. This production mechanism is enhanced by the  $D^{*0}\bar{D}^{*0} \rightarrow \gamma D^0 + \bar{D}^{*0} \rightarrow \gamma + X(3782)$  one loop triangle singularities producing a narrow peak at about the  $D^{*0}\bar{D}^{*0}$  threshold. E. Braaten, L.-P. He and K. Ingles have proposed a similar triangle singularity enhancement for the production of  $X(3782)$  and a photon using  $e^+e^-$  annihilation as the source of a  $D^{*0}\bar{D}^{*0}$  pair in a relative P-wave, which becomes possible because of its  $1^{++}$  quantum numbers [12]. Further related analysis on this regard may be found in Ref. [43, 44].

However, these methods focusing on the  $X(3782)$  production lack one important circumstance operating due to the finite resolution of the detectors, since they assume a *pure* ini-

tial mass state (mostly the bound state mass  $M_X$ ). In reality, any nearby initial states with the *same*  $1^{++}$  quantum numbers will produce a signal in the final state due to the finite resolution in the final state. We have reported recently on the neat and accurate cancellation between the would-be  $X(3782)$  bound state and the  $D\bar{D}^*$  continuum in the initial state which has a sizable impact on the final density of states and blurs the detected signal [14, 15]. In this work, we will extend those works to analyze the implications on the allegedly accurate mass determinations.

The similarities between  $d$  and  $X(3782)$  already noted in Refs. [45–47] have been corroborated on a quantitative level in our recent work [16], where we have pointed out that they are also applicable from the point of view of production at accelerators [16]. However, a crucial and relevant difference for the present work is that while the deuteron is detected *directly* by analyzing its track and/or stopping power leaving a well-defined trace, the  $X(3782)$  is inferred from its decay properties, mainly through the  $J/\psi\rho$  and  $J/\psi\omega$  channels.

### IV. LEVEL DENSITY IN THE $X(3782)$ CHANNEL

#### A. Coupled channel scattering

In order to implement the formula given by Eq. (2), we make some digression on the  $D\bar{D}^*$  scattering states in the  $1^{++}$ , which actually resembles closely the same channel for the deuteron. However, while the partial wave analysis of NN scattering data and the determination of the corresponding phase-shifts is a well-known subject, mainly due to the abundance of data [48], we remind that a similar analysis in the  $D\bar{D}^*$  case is, at present, in its infancy and thus our first analysis in Ref. [14] has been based on a quark-model. In the  $1^{++}$  channel, the presence of tensor force implies a coupling between the  $^3S_1$  and  $^3D_1$  channels, so that the S-matrix is given by

$$S^J = \begin{pmatrix} \cos \epsilon_j & -\sin \epsilon_j \\ \sin \epsilon_j & \cos \epsilon_j \end{pmatrix} \begin{pmatrix} e^{2i\delta_{j-1}^{1j}} & 0 \\ 0 & e^{2i\delta_{j+1}^{1j}} \end{pmatrix} \times \begin{pmatrix} \cos \epsilon_j & -\sin \epsilon_j \\ \sin \epsilon_j & \cos \epsilon_j \end{pmatrix}. \quad (10)$$

From here we define the T-matrix

$$S^J = 1 - 2ikT^J, \quad (11)$$

The S and D eigen phase-shifts have been shown in our previous work [14] using the quark cluster model of Ref. [49, 50] which includes both a  $c\bar{c}$  and  $D\bar{D}^*$  channels. The cumulative number is shown in Fig. 2. The outstanding feature is the turnover of the function as soon as a slightly non-vanishing  $c\bar{c}$  content in the  $X(3782)$  is included, unlike the purely molecular picture (see Ref. [14] for a more detailed discussion). We also compute the cumulative number for the coupled-channels EFT model of Ref. [51] fine-tuning the parameters to agree at low energies with the quark model. In both cases the fitting parameters have been binding properties

of the  $X(3872)$ . As we see, results present a rather similar pattern over the entire plotted energy range; the sharp rise of the cumulative number is followed by a strong decrease generated by the phase-shift. Moreover, we have checked that the S-wave phase-shift asymptotically approaches  $\pi$  (due to the bound  $X(3940)$ -state of the purely confined channel [50] which becomes a resonance when coupled to the  $D\bar{D}^*$  continuum) and hence  $N(\infty) = 1$  in agreement with the modified Levinson's theorem of interactions with confining channels [28].

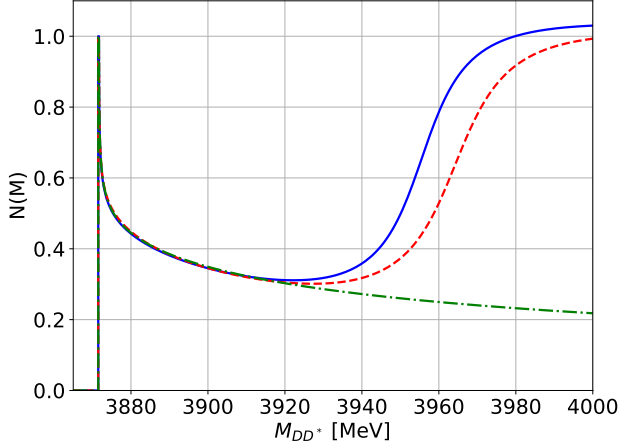


FIG. 2. Comparison between the cumulative number of the  $1^{++}$  sector with  $E_b = 180$  keV in different models: The coupled-channels EFT model of Ref. [51] with  $d = 0.4 \text{ fm}^{1/2}$ ,  $C = -976 \text{ fm}^2$  and  $m_{c\bar{c}}^{(0)} = 3947.44 \text{ MeV}$  (blue); the coupled-channels CQM model of Ref. [49] with  $m_{c\bar{c}}^{(0)} = 3947.44 \text{ MeV}$  and  $\gamma_{P_0} = 0.194$  (dashed red) and the Effective Range Approximation (ERA) model with  $r_0 = 1 \text{ fm}$  and  $a_s = \frac{1}{\sqrt{2\mu E_b}} = 10.58 \text{ fm}$  (dash-dot green).

### B. Effective range approximation

However, as we will see, the S-D waves mixing stemming from the tensor force has an influence for larger energies than those considered here [14]. Therefore, in order to illustrate how the cancellation comes about, we also considered a simple model which works fairly accurately for *both* the deuteron and the  $X(3872)$  by just considering a contact (Gaussian) interaction [52] in the  $^3S_1$ -channel and using effective range parameters to determine the corresponding phase-shift in the  $d$  and  $X(3872)$  [14, 53] respectively. The result for  $N(M)$  together with the EFT and CQM predictions can be seen in Fig. 2. Of course, if the binding energy is not that small, several effects appear and, in particular, the composite nature of the  $X(3872)$  becomes manifest (see e.g. [49]). All these similarities suggests the possibility of using the shape-independent Effective Range Approximation (ERA) to second order to calculate the phaseshifts near threshold. In ERA, we have that the  $\delta$  is given as a function

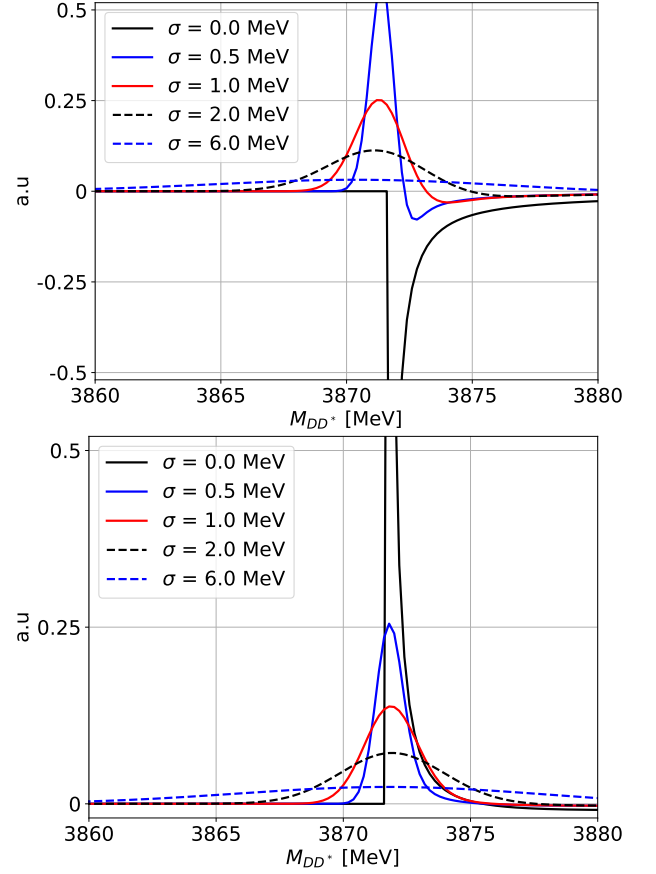


FIG. 3. Upper: Smeared density of states for  $E_b = 180$  keV for different resolutions. Lower: Same for  $E_b = -180$  keV (virtual).

of two parameters:

$$k \cot \delta = -\frac{1}{a_s} + \frac{1}{2} r_0 k^2 \quad (12)$$

where  $k$  is the CM momentum

$$k = \sqrt{2\mu(M - M_0)} \quad (13)$$

where  $\mu = M_D M_{D^*} / (M_D + M_{D^*})$  is the reduced mass and  $M_0 = M_D + M_{D^*}$  is the threshold mass. The comparison in Fig. 2 between ERA and the two coupled-channels models reassures the validity of the approximation for the range  $\sqrt{s} \lesssim 3920 \text{ MeV}$ . The partial wave inverse scattering amplitude is given by

$$f_0(k)^{-1} = k \cot \delta - ik \quad (14)$$

and, in general, bound and virtual states correspond to poles of  $f_0(k)$  at  $k = \pm i\gamma_X$  in the first and second Riemann sheet in energy  $E_b = M_X - M_0$  respectively. It is worth mentioning that Kang and Oller have comprehensively studied the pole structure and analyzed the character of the  $X(3872)$  in terms of bound and virtual states within simple analytical parameterizations [37], although the Dashen-Kane cancellation was not addressed.

Channel	$\sigma$	$\Delta m$	$\Delta M$	Reference
$J/\psi\pi^+\pi^-$	$1.14 \pm 0.07$	3	20	Ref. [54]
$J/\psi\pi^+\pi^-$	$3.33 \pm 0.08$	2	$6\sigma \approx 20$	Ref. [55]
$J/\psi\pi^+\pi^-$	4	2	18	Ref. [5]

TABLE I. Detector energy resolutions  $\sigma$ , binning  $\Delta m$  and energy window  $\Delta M$  in several experiments detecting  $X(3872)$  decays.

### C. Finite energy resolution

The detector response function transforms the monochromatic signal of mass  $M_X$  in a Gaussian distribution  $R_\sigma(M_X, m)$  with  $\sigma$  resolution [29]. It reflects the imperfection of the detector to measure a single energy due to the Poisson statistics of the energy deposition. The energy window  $\Delta M$  is interpreted as the energy range where the final channel products are selected as decay products of the  $X(3872)$  (and, thus, reconstructed). Usually they are taken as  $\pm(2-3)\sigma$ , to take most of the Gaussian distribution. The binning energy  $\Delta m$  corresponds to the actual sampling of discriminated data.

The experiments measure such Gaussian distributions, from where the typical resolution  $\sigma$  can be extracted. For example, in Ref. [54](page 4) the authors claim a resolution of  $\sigma \approx 1$  MeV when measuring the mass of the  $\psi(3686)$ , and  $J/\psi\pi\pi$  events between 3.86 and 3.88 GeV are selected, thus, employing an energy window of 20 MeV and binning with 3 MeV. The situation for this and other experiments [5, 55] is summarized in Table I (see appendix A for details).

According to Table I the finest value for the resolution  $\sigma$  is around  $\sigma = 1$  MeV, and it reflects the best possible experimentally accessible resolution at present. Additionally, the energy window of selected events would be of  $\Delta M = 20$  MeV.

### D. Smearing of the density of states

According to the general expression, Eq. 6, and neglecting the inessential S-D wave mixing at low energies, the density of states in the  $1^{++}$  channel for the bound  $X$  case is given by

$$\rho(m) = \delta(m - M_X) + \frac{1}{\pi} \delta'(m). \quad (15)$$

where the S-wave phase-shift as a function of the invariant mass vanishes below the  $DD^*$  threshold. For the unbound case, the bound state contribution  $\delta(m - M_X)$  is simply dropped out. Note that from Fig. 2 the phase-shift at low energies is a decreasing function, so its derivative becomes negative which is the essence of the Dashen-Kane cancellation. If the mass of  $X$  is not correctly reconstructed, because we have a finite resolution in our detector, given by the response function  $R_\sigma(m, M)$ , we will measure real  $DD^*$  pairs from the decay of the  $X$  and  $DD^*$  from the continuum, so that we cannot distinguish them due to the finite detector resolution. Thus, we have to fold the detector response function and the density of states as done in Eq. (5) applied

to the  $X(3872)$  case

$$\bar{\rho}_\sigma(M) = \Theta R_\sigma(M_X, M) + \frac{1}{\pi} \int_{M_{DD^*}}^{\infty} R_\sigma(m, M) \delta'(m) dm \quad (16)$$

being  $M_{DD^*}$  the  $DD^*$  threshold mass and  $\Theta \equiv \Theta(M_{DD^*} - M_X)$  the Heaviside function. We show in Fig. 3 the smear of the density of states for  $E_b = 180$  keV (bound) and  $E_b = -180$  keV (virtual) for different resolutions in the range  $\sigma = 1 - 6$  MeV. When  $E_b \gg \sigma$  the finite resolution does not modify the lineshape and effectively corresponds to  $\sigma \rightarrow 0$  picture. For finite  $\sigma$  the cancellation becomes rather evident and is more effective for larger resolutions  $\sigma \gg |E_b|$  where the difference between a bound and a virtual state becomes small.

### E. Missing decays vs missing counts

According to a recent work, there are a number (about a third) of unknown decays when absolute branching ratios are considered and compared to the total width of the  $X(3872)$  [56] (see also [57] for an experimental upgrade) suggesting new experiments to detect these missing decays. The statistical analysis carried out by the authors of Ref. [56] provides large error bars for the branching  $Br(X(3872) \rightarrow \text{unknown}) = 1 - \sum_i \Gamma_i / \Gamma = 31.9^{+18.1}_{-31.5} \%$  from the analysis of 8 detected channels (see their table II). Actually, about half of the decays goes into  $D\bar{D}^*$  pairs. We note here that the quenching effect we unveil here may be behind such missing decays, since quite generally and due to the Dashen-Kane cancellation the counted signals are suppressed against the original ones,  $\bar{N}_{1^{++}} < N_{X(3872)}$ . This undercounting is in complete agreement with our previous study [14, 15] on occupation numbers at finite temperature and of relevance in  $X(3872)$  in heavy ion-collisions. It also complies with the similarities of production rates at finite  $p_T$  of deuterons and  $X(3872)$  states in pp collisions at ultrahigh energies in the mid-rapidity region [16] which provides, after correcting the effect to a one-to-one production rate,  $N_X/N_d \sim 1$ .

## V. SMEARING OF LINESHAPES

### A. General considerations

As we have discussed above, the finite detector resolution does not separate between the signals triggered by a bound  $X(3872)$  and  $D\bar{D}^*$  pairs in the  $1^{++}$  nearby continuum. This fact in itself should not necessarily be a cause of concern if the level density was a smooth function within the finite resolution  $\sigma$ . However, we have seen that this is *not* what happens in the  $1^{++}$  channel; a relevant variation with positive and negative contributions does take place. This, of course, sets the problem on how would it be possible to deduce accurately the mass of the  $X(3872)$  state given these limitations on resolution and being aware of the cancellation effect.

In general, the direct determination of the mass would require more precision on the mass of the constituents (i.e.,

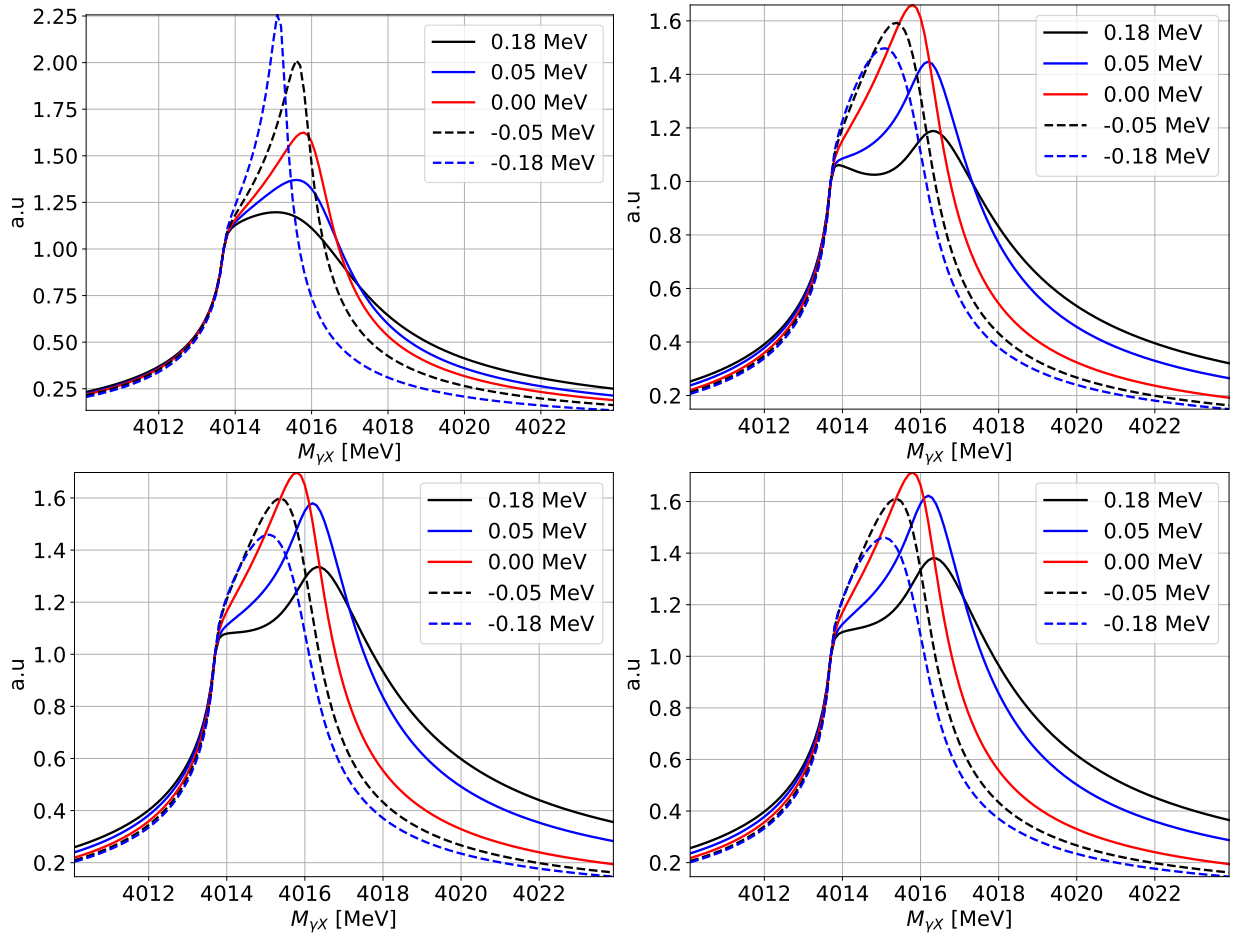


FIG. 4. Smeared lineshapes of states,  $\bar{L}(s)$ , for  $\sigma = 0$  MeV (top, left),  $\sigma = 1$  MeV (top, right),  $\sigma = 3$  MeV (bottom, left), and  $\sigma = 4$  MeV (bottom, right) for the S-wave source of Ref. [11], for different binding energies and a  $\Delta m = 2$  MeV.

$D^0$  and  $D^{*0}$  mass assuming a molecular nature) and a large acquisition of statistics, considering the small value of the  $X$  binding energy. An alternative, and more interesting method, is the characterization of production processes in terms of a suitable mass operator  $\mathcal{O}(M)$ , sensitive to small variations of the binding energy. Recently, two methods involving triangle singularities near the  $D^{*0}\bar{D}^{*0}$  threshold have been proposed [11, 12]. Those kinematic singularities, which are formed when the three particles composing the triangle are simultaneously on-shell, have been suggested to provide a more accurate method to determine the  $X(3872)$  binding energy than direct mass measurements.

### B. Smearing effects

All experimental analysis make a distinction between the resolution  $\sigma$  of the detectors leading to a gaussian response function for a monochromatic signal with invariant mass  $m_0$

$$\delta(m - m_0) \rightarrow \frac{1}{\sqrt{2\pi}\sigma} e^{-\frac{1}{2}\left(\frac{m-m_0}{\sigma}\right)^2} \quad (17)$$

This is one source of mixing mass effects. On the other hand, a choice of mass window,  $\Delta m$  for measurements must be made. This is another source of mass mixing, since the resulting signal will correspond to the averaged mass distribution around a chosen mass interval  $\pm\Delta m/2$ .

In order to illustrate the aforementioned limitations due to the resolution and the cancellation effect, let's consider now a general lineshape  $L(s, M)$ , where  $s$  is the invariant mass and  $M$  is the reconstructed mass of the secondary  $X$  particle from the Gaussian distribution  $R_\sigma(m, M)$ . The convoluted lineshape from the  $X$  particle with mass  $M$  is (Eq. 9)

$$\bar{L}(s) = \Theta \mathcal{R}(M_X) L(s, M_X) + \frac{1}{\pi} \int_{M_{DD^*}}^{\infty} \mathcal{R}(m) L(s, m) \delta'(m) dm \quad (18)$$

with  $\mathcal{R}(m) = \frac{1}{2\Delta m} \left[ \text{Erf}\left(\frac{m-M_X+\Delta m/2}{\sqrt{2}\sigma}\right) + \text{Erf}\left(\frac{M_X-m+\Delta m/2}{\sqrt{2}\sigma}\right) \right]$ .

We analyze the effect of smearing for the lineshapes generated in the  $X(3872)\gamma$  production process using either a relative S-wave [11] or P-wave [12] source of a  $D^{*0}\bar{D}^{*0}$  pair. Results for the S-wave source of Ref. [11] can be seen in Fig. 4 and results for the P-wave source of Ref. [12] are shown in



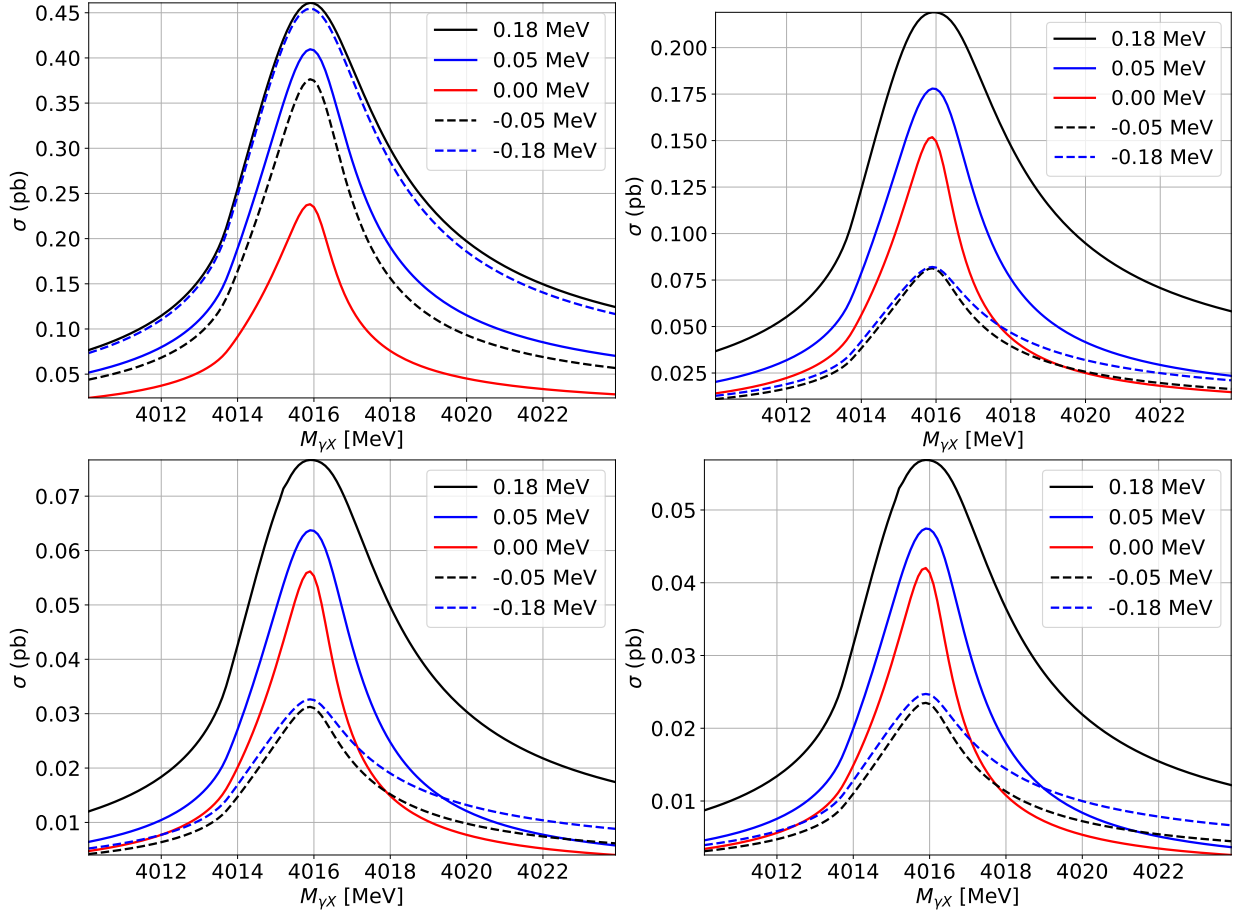


FIG. 5. Smeared lineshapes of states,  $\bar{L}(s)$ , for  $\sigma = 0$  MeV (top, left),  $\sigma = 1$  MeV (top, right),  $\sigma = 3$  MeV (bottom, left), and  $\sigma = 4$  MeV (bottom, right) for the P-wave source of Ref. [12], for different binding energies and a  $\Delta m = 2$  MeV.

Fig. 5, without considering a finite binning in the  $\gamma X$  invariant mass spectrum. For the S-wave source, normalized to the  $D^{*0}\bar{D}^{*0}$  threshold, we appreciate a change in the shape of the distribution, which pretty much blurs the neat distinction due to the  $X$  binding energy. Still, we see a separation of the lineshape tails which could be used for the latter purposes. The cancellation and the finite resolution, thus, leads to a more complicated precise measurement of the  $X(3872)$  mass, specially when finite statistics are considered (see discussion below). For the P-wave source, the main effect is the absolute value decreases of the lineshapes, depending on their binding energy due to the cancellation (effect that also occurs for the S-wave source but it not appreciated due to the normalization of the lineshapes).

### C. Finite samples

It is interesting to analyze the S-wave source results from the counting statistics point of view. We expect a convergence of all  $\gamma X$  lineshapes regardless of the  $X$  binding energy. Their tails decrease at different rates, but a limited statistics can compromise their proper identification. Quite generally we

will be able to discern two different (smeared) signals if the number of events fulfills

$$\frac{\Delta\sigma}{\sigma} \sim \frac{1}{\sqrt{N}} \quad (19)$$

In Fig. 6 we show an example of limited resolution for binding energies  $E_b = 180$  keV and  $E_b = -180$  keV (virtual), a  $\sigma = 2$  MeV and an energy bin of  $E_{\text{win}} = 1$  MeV. The synthetic data is obtained by randomly sampling  $N = 100$  and 1000 events in the  $[4010, 4020]$  energy range, according to the probability density function given by the lineshapes of Fig. 4(bottom). As the global normalization of the lineshapes of Fig. 4 are not known, the same occurs to the global normalization of the synthetic data, so caution should be taken when direct comparing between the lineshapes for different binding energies. Of course, for larger values of  $\sigma$  all curves resemble each other and the strong mass dependence is largely washed out. We believe these effects should be considered in an eventual benchmark experimental determination of the  $X(3872)$  mass.



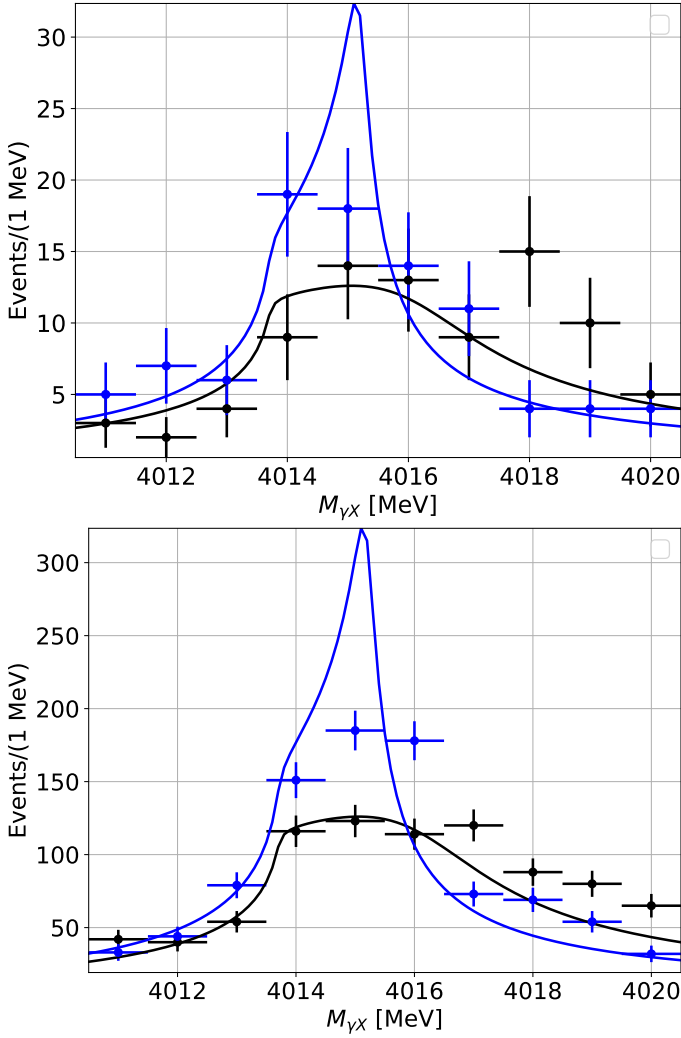


FIG. 6. Binned smeared lineshapes of the S-wave source for  $N = 100$  events (top) and  $N = 1000$  events (bottom). We compare the  $E_b = 180$  keV (black) and  $E_b = -180$  keV (blue) binding energies, using a  $\sigma = 2$  MeV resolution, an energy bin of 1 MeV and a  $\Delta m = 2$  MeV. The full lineshape corresponding to  $\Delta M = \sigma = 0$  is shown for comparison.

## VI. BINDING INDEPENDENT SHORT DISTANCE $\bar{D}D^*$ CORRELATIONS

One important aspect within the present context is that, regardless of the precise features of the lineshape, the existence of the peak does not depend crucially on the  $X(3872)$  being truly bound or unbound. At long distances the reduced relative wave functions for a bound/unbound  $X(3872)$  state behaves as

$$u_X(r) \rightarrow A_X e^{\mp \gamma_X r} \quad (20)$$

respectively where  $\gamma_X$  is the corresponding wave number which corresponds to a pole of the partial wave amplitude. Clearly, since the signal for the  $X(3872)$  is reconstructed by detecting its weak decay products, which involves a short distance operator and tells us about the relative  $\bar{D}D^*$  wave

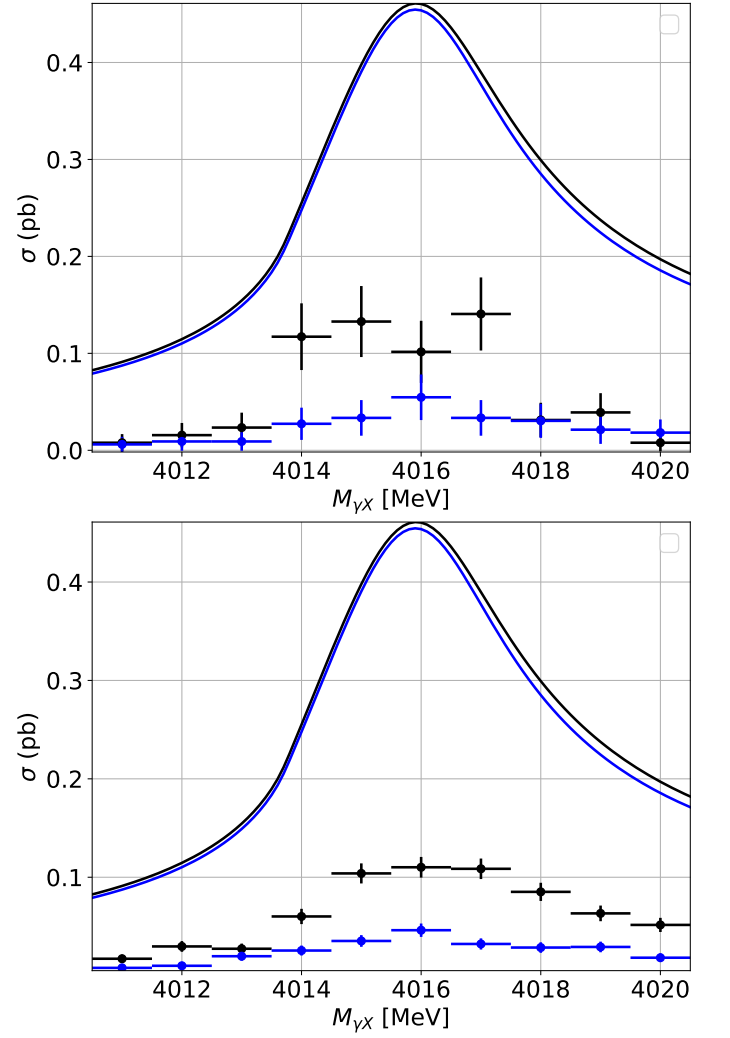


FIG. 7. Binned smeared lineshapes of the P-wave source for  $N = 100$  events (top) and  $N = 1000$  events (bottom). Same legend as in Fig. 6.

function at *short distances*. To further analyze this issue, we plot in Fig. 8 the case of bound/unbound wave functions, normalized so that their long-distance extrapolated value to the origin is unity, i.e.  $u_X(r) \rightarrow e^{\mp \gamma_X r}$ , using for illustration the particular (unquenched) quark model of Ref. [49, 50] which includes both a  $c\bar{c}$  and  $\bar{D}D^*$  channels in the description of the  $X(3872)$  state. As we see, their short distance behaviour is nearly identical although they are completely different at long distances<sup>1</sup>. Thus, the bumps found experimentally and attributed to be the  $X(3872)$  are certainly reflecting a strong short distance correlated  $\bar{D}D^*$  pair in the  $1^{++}$  channel, and not just a bound state feature. The short distance dominance

<sup>1</sup> Remarkably, these features between bound or unbound  $X(3872)$  are also present in the neutron-proton case; while in the triplet  $^3S_1$  channel they form a bound state, in the singlet  $^1S_0$  channel they are unbound. Nevertheless, their wave functions are rather similar at short distances (see e.g. [58] for a discussion).

of the  $X(3872)$  is not new, and it provides an explanation for the large isoscalar to isovector decay modes (see e.g. [52]).

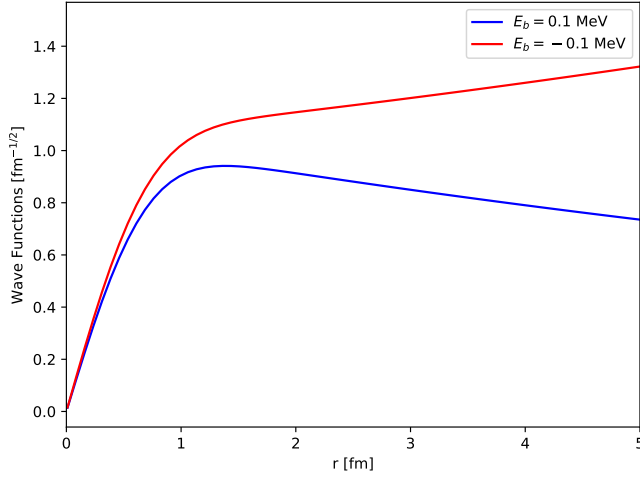


FIG. 8. Reduced  $\bar{D}D^*$  S-wave function for the  $1^{++}$  channel in the quark model of Ref. [49, 50]. We compare for the bound case with  $E_b = 180$  keV (blue) and the unbound case with  $E_b = -180$  keV (red) binding energies as a function of the relative  $\bar{D}D^*$  distance.

## VII. CONCLUSIONS

In this paper, we have analyzed the impact of finite detector resolution in the production and decay of the  $X(3872)$

state. We have discussed the cancellation effect due to the superposition in the level density in the  $1^{++}$  channel of bound state and nearby  $\bar{D}D^*$  continuum states in the initial state, which cannot be separated in the final state when the binding energy is much smaller than the energy resolution. Our results suggest that the mechanism of production of weakly bound states such as the  $X(3872)$  undercounts the number of states  $\bar{N}_{1^{++}} < N_{X(3872)}$ , an effect which is in harmony with the missing resonances reported in a recent absolute branching ratio analysis. This signal suppression is in complete agreement with our previous study on occupation numbers at finite temperature and of relevance in  $X(3872)$  in heavy ion-collisions. It also complies with the deuteron to  $X(3872)$  finite  $p_T$  production ratio in pp collisions at ultrahigh energies at mid-rapidity. Our findings are also relevant to future benchmark determinations of the  $X(3872)$ , particularly those displayed by the strong lineshape dependence in production processes involving triangle singularities. Quite generally we find that the initial density of states triggering a signal of  $X$ -production in a finite resolution energy detector blurs the spectrum and hence the strong mass dependence is reduced and could only be pinned down with sufficiently high statistics. This is in harmony with the relevance of short distance  $\bar{D}D^*$  correlations in the  $1^{++}$  channel. We expect our observations to hold in similar weakly bound states not directly measured through their track, but inferred from their decay products.

- 
- [1] P.Z. et al. (Particle Data Group), Prog. Theor. Exp. Phys. (2020) 083C01.
  - [2] E. Ruiz Arriola et al., Excited Hyperons in QCD Thermodynamics at Freeze-Out, pp. 128–139, 2016, 1612.07091.
  - [3] Belle, S.K. Choi et al., Phys. Rev. Lett. 91 (2003) 262001, hep-ex/0309032.
  - [4] BaBar, B. Aubert et al., Phys. Rev. D71 (2005) 031501, hep-ex/0412051.
  - [5] Belle, S.K. Choi et al., Phys. Rev. D 84 (2011) 052004, 1107.0163.
  - [6] LHCb, R. Aaij et al., Phys. Rev. Lett. 110 (2013) 222001, 1302.6269.
  - [7] S. Godfrey and S.L. Olsen, Ann. Rev. Nucl. Part. Sci. 58 (2008) 51, 0801.3867.
  - [8] F.K. Guo et al., Rev. Mod. Phys. 90 (2018) 015004, 1705.00141.
  - [9] N. Brambilla et al., (2019), 1907.07583.
  - [10] LHCb, R. Aaij et al., JHEP 08 (2020) 123, 2005.13422.
  - [11] F.K. Guo, Phys. Rev. Lett. 122 (2019) 202002, 1902.11221.
  - [12] E. Braaten, L.P. He and K. Ingles, Phys. Rev. D100 (2019) 031501, 1904.12915.
  - [13] R.F. Dashen and G.L. Kane, Phys. Rev. D11 (1975) 136.
  - [14] P.G. Ortega et al., Phys. Lett. B781 (2018) 678, 1707.01915.
  - [15] P.G. Ortega and E. Ruiz Arriola, PoS Hadron2017 (2018) 236, 1711.10193.
  - [16] P.G. Ortega and E. Ruiz Arriola, Chinese Physics C 43 (2019) 124107, 1907.01441.
  - [17] E. Ruiz Arriola and P.G. Ortega, 12th International Winter Workshop "Excited QCD" 2020, 2020, 2005.01531.
  - [18] E. Beth and G. Uhlenbeck, Physica 4 (1937) 915.
  - [19] R. Dashen, S.K. Ma and H.J. Bernstein, Phys. Rev. 187 (1969) 345.
  - [20] R.F. Dashen and R. Rajaraman, Phys. Rev. D10 (1974) 694.
  - [21] R.F. Dashen and R. Rajaraman, Phys. Rev. D10 (1974) 708.
  - [22] P.M. Lo, Eur. Phys. J. C 77 (2017) 533, 1707.04490.
  - [23] P.M. Lo, (2020), 2007.03392.
  - [24] N. Fukuda and R. Newton, Phys. Rev. 103 (1956) 1558.
  - [25] B.S. DeWitt, Phys. Rev. 103 (1956) 1565.
  - [26] M. Gómez-Rocha and E. Ruiz Arriola, Phys. Lett. B 800 (2020) 135107, 1910.10560.
  - [27] M. Gómez-Rocha and E. Ruiz Arriola, Phys. Rev. D 101 (2020) 036003, 1911.08990.
  - [28] R.F. Dashen, J.B. Healy and I.J. Muzinich, Phys. Rev. D14 (1976) 2773.
  - [29] G.F. Knoll, Radiation detection and measurement (John Wiley & Sons, 2010).
  - [30] E. Ruiz Arriola, L.L. Salcedo and E. Megias, Acta Phys. Polon. Supp. 8 (2015) 439, hep-ph/1505.02922.
  - [31] E. Ruiz Arriola, L.L. Salcedo and E. Megias, Acta Phys. Polon. B45 (2014) 2407, hep-ph/1410.3869.

- [32] C.J. Horowitz and A. Schwenk, Nucl. Phys. A776 (2006) 55, nucl-th/0507033.
- [33] S. Nussinov and D.P. Sidhu, Nuovo Cim. A44 (1978) 230.
- [34] Particle Data Group, M. Tanabashi et al., Phys. Rev. D98 (2018) 030001.
- [35] A. Esposito, A. Pilloni and A.D. Polosa, Phys. Rept. 668 (2016) 1, 1611.07920.
- [36] M. Karliner, J.L. Rosner and T. Skwarnicki, (2017), 1711.10626.
- [37] X.W. Kang and J.A. Oller, Eur. Phys. J. C77 (2017) 399, 1612.08420.
- [38] E. Braaten and M. Lu, Phys. Rev. D76 (2007) 094028, 0709.2697.
- [39] R. Karplus, C.M. Sommerfield and E.H. Wichmann, Phys. Rev. 111 (1958) 1187.
- [40] A.P. Szczepaniak, Phys. Lett. B747 (2015) 410, 1501.01691.
- [41] E. Oset et al., Few Body Syst. 59 (2018) 85.
- [42] X.H. Liu, M. Oka and Q. Zhao, Phys. Lett. B753 (2016) 297, 1507.01674.
- [43] S. Sakai, E. Oset and F.K. Guo, Phys. Rev. D 101 (2020) 054030, 2002.03160.
- [44] R. Molina and E. Oset, Eur. Phys. J. C 80 (2020) 451, 2002.12821.
- [45] N.A. Tornqvist, Z. Phys. C61 (1994) 525, hep-ph/9310247.
- [46] F.E. Close and P.R. Page, Phys. Lett. B578 (2004) 119, hep-ph/0309253.
- [47] E. Braaten and M. Kusunoki, Phys. Rev. D69 (2004) 074005, hep-ph/0311147.
- [48] R. Navarro Pérez, J. Amaro and E. Ruiz Arriola, Phys. Rev. C 88 (2013) 064002, 1310.2536, [Erratum: Phys.Rev.C 91, 029901 (2015)].
- [49] P.G. Ortega et al., Phys. Rev. D81 (2010) 054023, hep-ph/0907.3997.
- [50] P.G. Ortega, D.R. Entem and F. Fernandez, J. Phys. G40 (2013) 065107, hep-ph/1205.1699.
- [51] E. Cincioglu et al., Eur. Phys. J. C76 (2016) 576, 1606.03239.
- [52] D. Gamermann et al., Phys. Rev. D81 (2010) 014029, hep-ph/0911.4407.
- [53] E. Ruiz Arriola, S. Szpigel and V. Timoteo, Phys. Lett. B 728 (2014) 596, 1307.1231.
- [54] BESIII, M. Ablikim et al., Phys. Rev. Lett. 112 (2014) 092001, 1310.4101.
- [55] LHCb, R. Aaij et al., Eur. Phys. J. C 72 (2012) 1972, 1112.5310.
- [56] C. Li and C.Z. Yuan, Phys. Rev. D 100 (2019) 094003, 1907.09149.
- [57] BaBar, J. Lees et al., Phys. Rev. Lett. 124 (2020) 152001, 1911.11740.
- [58] A. Calle Cordon and E. Ruiz Arriola, Phys. Rev. C 78 (2008) 054002, 0807.2918.

### Appendix A: Details on the choice of resolution

In this section we come to justify the numbers provided in Table I.

- In Ref. [5], the authors make studies of the  $\psi' \rightarrow \pi^+\pi^-J/\psi$  as control sample using  $3.635\text{GeV} \leq M(\pi^+\pi^-J/\psi) \leq 3.735\text{GeV}$  and, for  $X(3872)$  studies, they use  $3.77\text{GeV} \leq M(\pi^+\pi^-J/\psi) \leq 3.97\text{GeV}$ . They select events in the range  $|M(\pi^+\pi^-J/\psi) - M_{\text{peak}}| \leq 0.009\text{ GeV}$ , taking energy bins of  $\Delta m = 2\text{ MeV}$ . The  $M(\pi^+\pi^-J/\psi)$  mass resolution of the Belle detector in the mass region of the  $X(3872)$  is claimed to be  $\sigma \simeq 4\text{ MeV}$ , larger than the  $X(3872)$  width estimation calculated in the work of  $\Gamma(X(3872)) < 1.2\text{ MeV}$  at 90% CL.
- Ablikim *et al* [54] analyze the angular distribution of the radiative photon in the  $e^+e^-$  CM frame and the  $\pi^+\pi^-$  invariante mass distribution. For the  $X(3872)$  signal, they select events between  $3.86\text{GeV} < M(\pi^+\pi^-J/\psi) < 3.88\text{ GeV}$ . The mass resolution of the detector is estimated from fits to the  $\psi(3686)$  signal, obtaining  $\sigma = (1.14 \pm 0.07)\text{ MeV}/c^2$ . Results are shown with an energy bin of  $\Delta m = 3\text{ MeV}$ .
- In Ref. [55], Aaij *et al* study the inclusive production of the  $X(3872)$  in pp collisions at  $\sqrt{s} = 7\text{ TeV}$ . Candidates are selected within a  $\pm 3\sigma$  energy window, where the mass resolution is estimated as  $\sigma = (3.33 \pm 0.08)\text{ MeV}$  for the  $X(2872)$ , so  $\Delta M \simeq 20\text{ MeV}$ . The energy bin used in the work is  $\Delta m = 2\text{ MeV}$ .